SPE calibration and other studies of the muon veto PMTs in DEAP-3600

Ameen Ismail

22 August 2017

Abstract

DEAP-3600 is a direct dark matter search employing 3600 kilograms of scintillating liquid argon contained within an acrylic vessel, which is viewed by 255 photomultiplier tubes (PMTs). Cosmogenic muons can induce neutron backgrounds through spallation. The muon veto system consists of 48 PMTs that detect Cherenkov light emitted by muons passing through the water tank that surrounds the detector. This is a summary of my work completed in the summer of 2017 under Dr. Kevin Graham. A single photoelectron (SPE) calibration was obtained for the functioning muon veto PMTs. qPE distributions were produced for some real runs and some Monte Carlo simulations. Additionally, the rate of events that triggered the muon veto PMTs is calculated for individual runs over a course of six months. Events that triggered the muon veto system which were followed by an event in the acrylic vessel are examined.

Contents

1 Introduction

DEAP-3600 aims to detect weakly interacting massive particles (WIMPs), a potential dark matter candidate. Elastic scattering of WIMPs off the 3600 kilograms of liquid argon contained within the acrylic vessel (AV) of the detector would produce scintillation light, which can be measured by the 255 photomultiplier tubes (PMTs) facing the AV [2]. As the experiment is located 2 kilometres underground, most incoming particles from cosmic rays never reach the detector. Nevertheless, cosmogenic muons can induce neutron backgrounds via nuclear spallation. For this reason, it is important to be able to distinguish muons from other events, so that one can rule out any events that follow as candidate WIMPs [5].

To this end the detector is surrounded by a water tank. Cosmogenic muons passing through produce Cherenkov radiation, which can be detected by 48 muon veto PMTs on the outer surface of the detector [3]. This report is a summary of the work I did on the muon veto system in the summer of 2017 under Dr. Kevin Graham. Much of this work built on Andrew Zwaniga's honours project (see [5]). As such, a sizeable portion is dedicated purely to reproducing Andrew's plots with newer data.

The veto PMTs each have a unique ID ranging from 0 to 47. PMTs 12, 32, and 34 are malfunctioning. Much of the analysis here depends on the variable muonVetoN, which refers to the number of muon veto PMTs that were triggered in an event. A PMT counts as triggered if, during an event, the digitized waveform for that PMT drops at least 10 ADC below the baseline value. Note that the expected baseline for each PMT is about 3900 ADC. Incidentally, there are 192 samples in each digitized waveform.

It is desirable to have a single photoelectron (SPE) calibration for the veto PMTs; that is, a measurement of the mean charge deposited into each PMT by a single photoelectron. This allows the computation of qPE, an estimate of the number of photoelectrons corresponding to a single event. qPE is defined for a single event as the sum over all relevant PMTs of charge deposited divided by mean SPE charge. Obtaining an SPE calibration for the muon veto PMTs was the primary goal of my research. It involved gathering data on muon events, analyzing the raw waveforms, producing SPE charge distributions and fitting them, and producing qPE distributions. A secondary purpose was to reproduce several of Andrew's plots. This involved producing plots of event rate and qPE-fprompt plots of muon veto (MV) events that were followed by acrylic vessel (AV) events.

2 Methods

The ROOT macros used in this study, as well as all the relevant data files and images, are indexed on my TWiki page at `https://www.snolab.ca/deap/private/TWiki/bin/view/Main/AISummary`.

2.1 Muon events

A list of 100,000 muon events were obtained by searching through physics runs from January 2017 to April 2017 for events with muonVetoN ≥ 2. Note that such events are sufficiently common that all 100,000 events came from the first run searched, run 19123. Run number, subrun number, event ID, and muonVetoN were recorded for each event. Similar lists were produced for runs 19517 (a physics run), 19523 (a uranium-232 (^{232}U, referred to as Th in some plot, since it decays to ^{232}Th) run), and run 19572 (a sodium-22 (^{22}Na) run), which were used only to produce qPE distributions. Later, when events with higher muonVetoN were required, runs from November 2016 to April 2017 were searched for events with muonVetoN ≥ 10.

In addition to the muonVetoN cut, some other cuts were applied:

!(calcut & 0x31f8) && !(dtmTrigSrc & 0x2) && (dtmTrigSrc & 0x80) && (dtmTrigOut & 0x1)

The calcut cut is a low-level cut that removes events unfit for physics analysis. For more details see [4]. The other two cuts remove PPG events (also not suitable for analysis) and events that did not trigger the muon veto detectors. These cuts are all similar or identical to those employed in [5].

2.2 Raw waveforms

About 100 raw waveforms were visualized. This was a preliminary step which motivated the thresholds and cutoffs used in the algorithms to find pulse regions and peaks. An example waveform is included below.

2.3 Analysis of waveform data

The raw waveforms corresponding to the list of 100,000 muon events were analyzed to extract the baseline value, RMS error on the baseline, pulse start and pulse end (if any), pulse height, pulse charge, and the number of peaks in each waveform. It was also recorded in which veto PMT each waveform was observed. In total, 2,631,528 waveforms were analyzed.

The start of a pulse region was identified by searching through the waveform for a waveform bin of less than 3900 ADC which was more than 2 ADC below the previous one. The end of a pulse region was identified in a similar fashion, but iterating in the opposite direction over the waveform. A single pulse region is identified for each waveform, even those with multiple pulses, in which case it extends from the beginning of the first pulse to the end of the last pulse. Also, note that many waveforms have no pulses at all.

The baseline of the waveform was calculated by averaging all waveform bins outside of the pulse region. The charge was then calculated as the negative of the baseline-subtracted integral over the pulse region. (The negative is required because pulses tend downward—see Figure 1). As a consequence of the baseline calculation method, the charge is the same whether the integral is taken over the pulse window or over the entire waveform. The pulse height was taken as the maximum downward deviation of the waveform from the baseline.

Peak finding was only employed over the pulse region. A peak was defined as a waveform bin at least 5 ADC below baseline, with a lower ADC value than the bin preceding or following it.

Identical analyses were performed for the other muon event lists described previously. The data were written to TTrees which may be found on the Carleton cluster at `$DEAPHOME/user/aismail/allData/analysis/`. The code used for analysis may be found at `$DEAPHOME/user/aismail/analyzeManyMuonEvents/analyzeManyMuonEvents_v4.cxx`.

2.4 Plotting and fitting

Histograms of the baseline waveform value were produced separately for each PMT and fitted to a Gaussian distribution. These involved only the analysis data corresponding to the first list of 100,000 events. Histograms of charge and height were also produced, broken down in muonVetoN ranges. This required the inclusion of waveforms corresponding to the high muonVetoN event list. Charge histograms

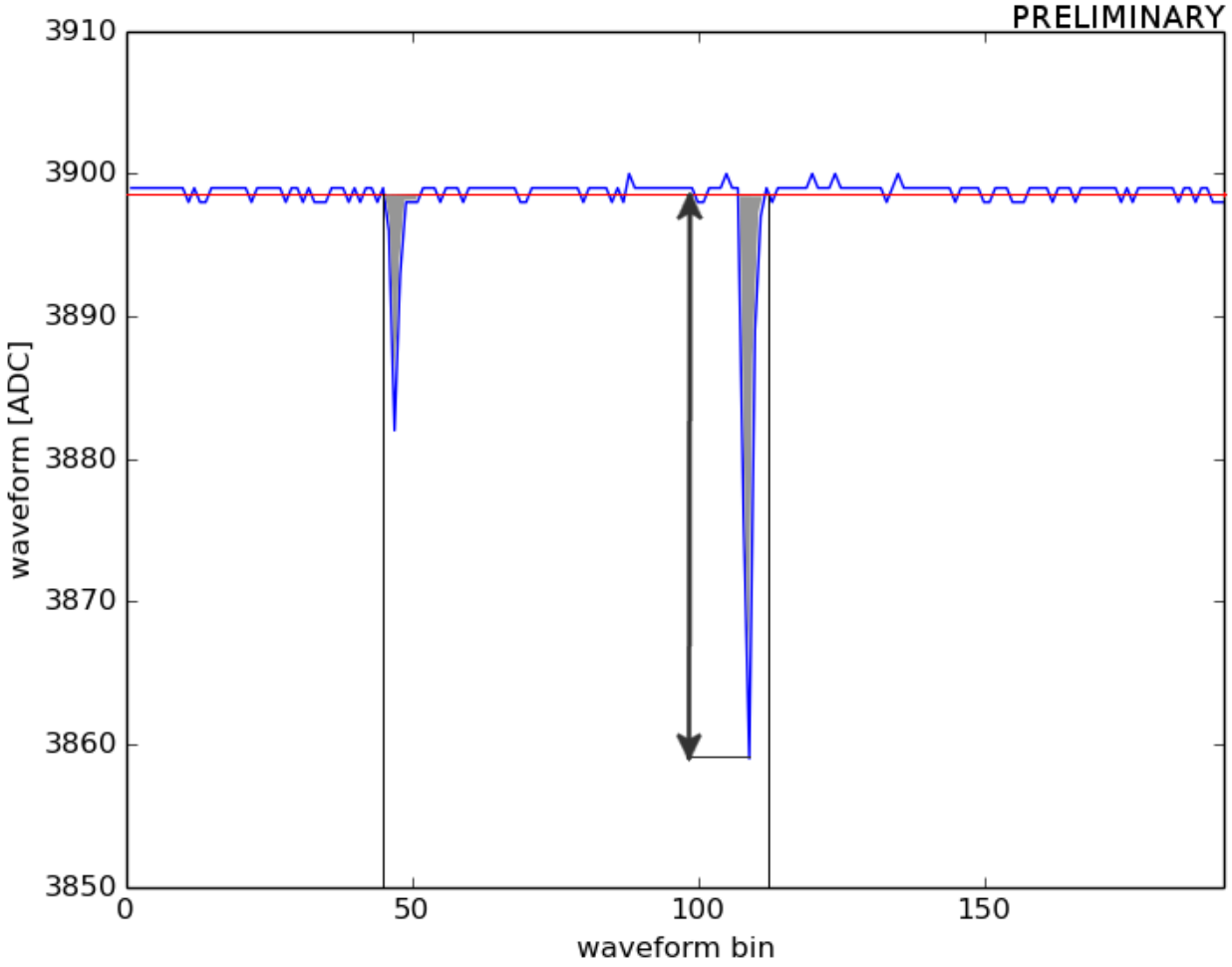

Figure 1: Sample waveform from a triggered muon veto PMT. The waveform trace is in blue. The red line indicates the baseline value of the waveform. Vertical black lines indicate the pulse region start and end. Vertical arrow indicates pulse height. The charge of this waveform is the area shaded in gray. This waveform has two peaks.

were also produced by categorizing waveforms by the number of peaks in the waveform. Waveforms from the malfunctioning PMTs were excluded from all charge and height histograms. Lastly, waveforms with a pulse region beginning in the first ten waveform bins or ending in the last ten bins were cut, because the baseline calculation, and therefore the charge and pulse height, are less reliable in these waveforms.

SPE charge distributions were produced for each PMT by only including waveforms with exactly one peak that correspond to events with muonVetoN < 20. These cuts, motivated by the charge plots described in the previous paragraph, were chosen to minimize contamination from multi-PE events. SPE charge distributions were fitted to a sum of two gamma distributions. This is the model used to calibrate the AV PMTs without the exponential, pedestal component [1]. In these fits, one gamma distribution always had a much greater amplitude than the other. The mean of the dominating gamma distribution was taken as the mean SPE charge.

2.5 qPE distributions

Using these mean SPE charges, qPE distributions were produced for the three runs described earlier: a physics run, a ^{232}U run, and a ^{22}Na run. 25000 events were sampled from each run. The distributions were normalized for livetime.

qPE distributions were also made for Monte Carlo simulations of various sources: ^{232}U (2.6 MeV gamma rays, 2 million events), AmBe (4.4 MeV gamma rays, 1 million events), and 3 GeV electrons (1000 events). Lastly, a qPE distribution was produced for the MV events followed by an AV event, as described in the next subsection.

2.6 Event rate and followers

The rate of muon events was calculated for physics runs from January 2017 to April 2017, as well as for several AmBe, ^{22}Na, and ^{232}U runs. Events were only counted if they satisfied muonVetoN ≥ 10 as well as the low-level cuts described earlier. This was repeated with a cut of muonVetoN ≥ 20.

Andrews FindMuonFollowers_v3 program was run on the physics data from November 2016 to April 2017, to search for muon veto (MV) events with muonVetoN ≥ 10 that were followed within 1 ms by an event in the AV. This was primarily to reproduce one of Andrews plots with newer data. The time delay between MV-AV event pairs was examined for pairs with AV event qPE ≥ 50000. This cut was chosen based on Andrew's lower bound on qPE for muons passing through the AV [5]. The MV events found were also used to make a qPE distribution (see above). For more details of the FindMuonFollowers_v3 program, see [5].

Lastly, physics runs from November 2016 to April 2017 were searched for coincident MV-AV events; that is, events that triggered both the MV PMTs and the AV PMTs. Again, this was an effort to reproduce Andrew's plots. The same low-level cuts described earlier were applied here as well.

3 Results

Note that many of these plots were produced for every veto PMT or every functioning veto PMT. For such plots, two sample figures are included. The location of plots for all veto PMTs is indexed at `https://www.snolab.ca/deap/private/TWiki/bin/view/Main/AISummary`.

3.1 Baseline

Sample baseline histograms are shown in Figure 2. The mean baselines are clustered tightly around a mean of approximately 3900 ADC. Figure 3 summarizes the mean and width of the Gaussian fit for each veto PMT, along with the RMS of the baseline distribution.

3.2 Charge and height

Charge and height distributions were made for waveforms from events that fell into specific muonVetoN ranges: 0-9, 10-19, 20-29, 30-39, and 40-45, all inclusive. The upper bound of 45 in the last range is due to the three malfunctioning PMTs. These are shown in Figure 4. Note that only waveforms with 0 or 1 peak

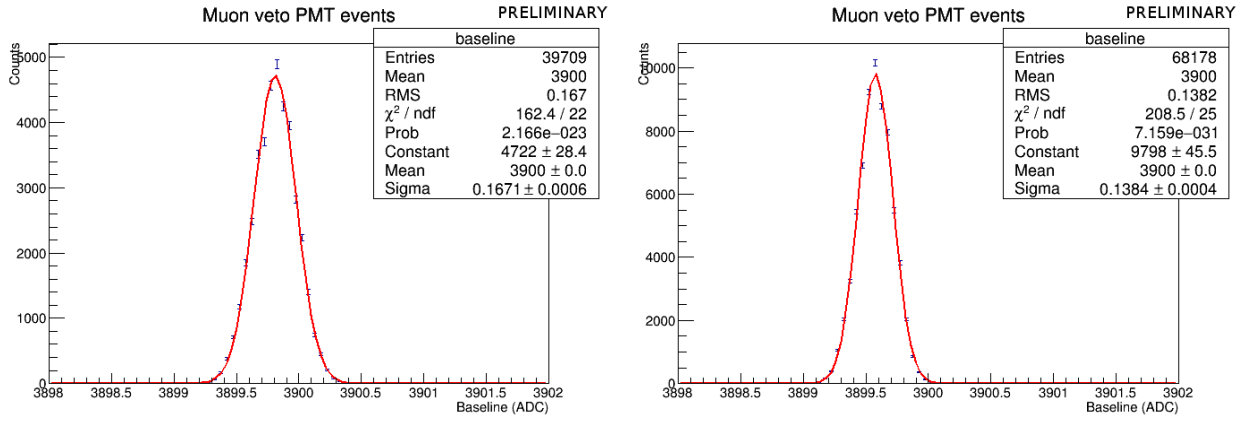

(a) Veto PMT ID 0.

(b) Veto PMT ID 24.

Figure 2: Distribution of the baseline in waveforms for two PMTs, fitted to a Gaussian distribution.

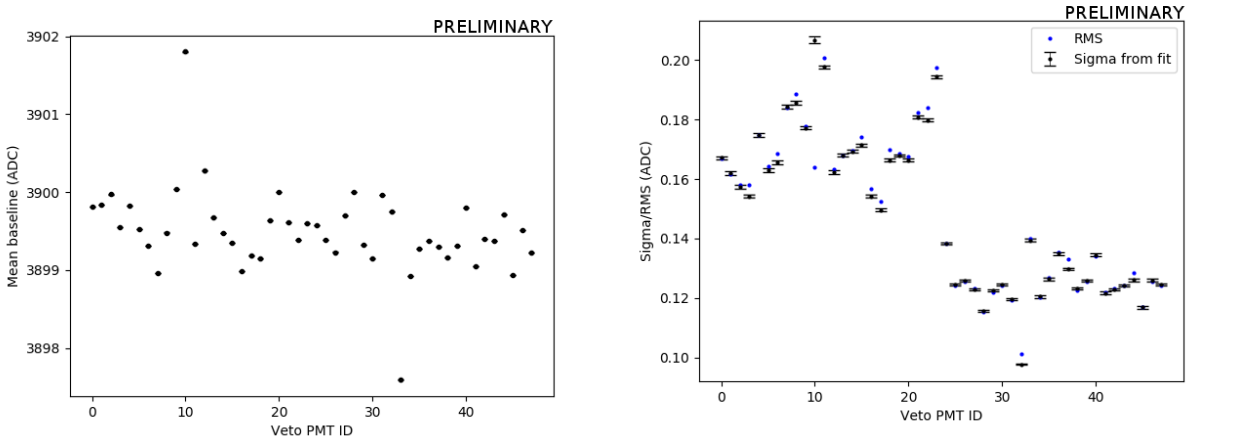

(a) The mean of the Gaussian for each veto PMT.

(b) Standard deviation (sigma) of the Gaussians and the RMS of the baseline distributions.

Figure 3: Summmary of properties of baseline distributions and the Gaussians fitted to them. Some error bars are too small to be seen.

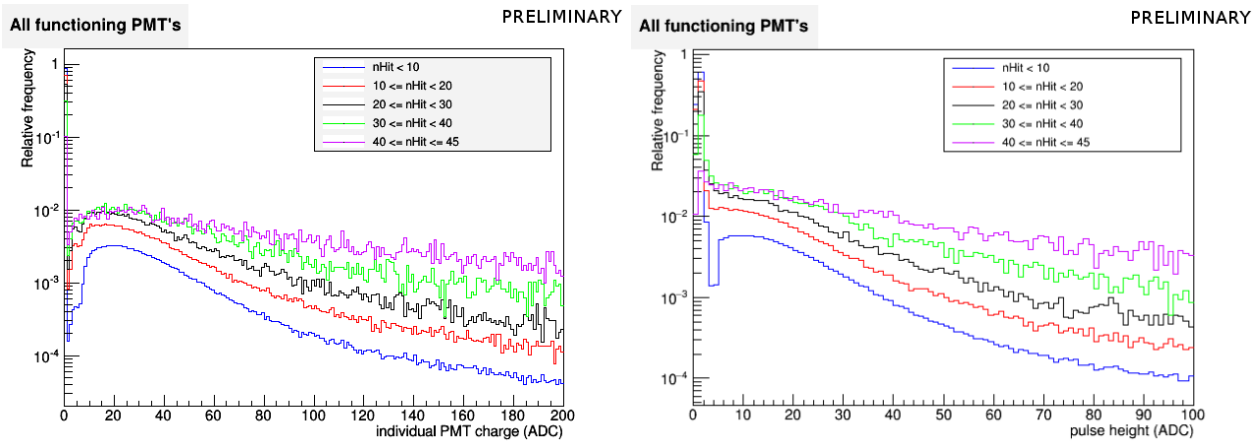

(a) Pulse charge.

(b) Pulse height.

Figure 4: Distributions of pulse charge and pulse height, over all PMTs, for waveforms corresponding to events in different muonVetoN (termed nhit in legend) ranges.

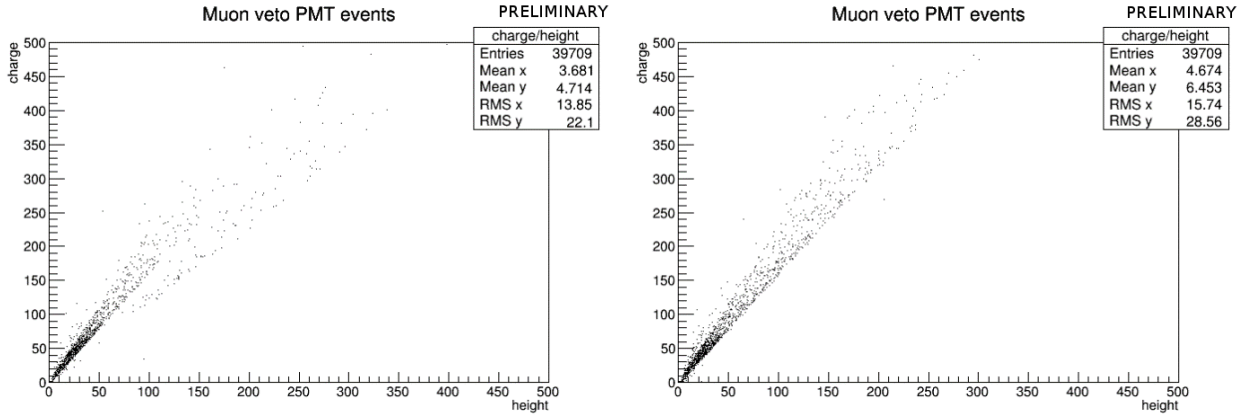

(a) Veto PMT ID 2.

(b) Veto PMT ID 5.

Figure 5: Pulse charge and pulse height in two PMTs. Note the close correlation.

are plotted. In general, waveforms with a higher charge and height are more likely to be found in events with higher muonVetoN. Furthermore, charge and pulse height are closely correlated, as evidenced by Figure 5. Figure 6 shows charge distributions for waveforms with different numbers of peaks. As the number of peaks increases the distribution becomes progressively more skewed to the right, ostensibly due to the increased contribution of multi-PE events. This is similar to the trend seen with increasing muonVetoN.

3.3 SPE Charge

Given the charge plots, SPE charge distributions were constructed only from waveforms with a single peak and muonVetoN < 20, so as to minimize multi-PE contamination. As with the charge and height plots, waveforms with early or late pulses were discarded. Two sample SPE charge distributions, fitted to the sum of two gamma distributions as described earlier, are provided below (Figure 7). The mean SPE charge was taken as the mean of the dominating gamma distribution. These are plotted in Figure 8, which also includes two values for mean charge in each PMT: one calculated by myself from the same data used to produce the previous plots, and the other calculated by Che Geofroy from AARF data (see [3]). The mean SPE charges are consistently lower than the mean charges. The reduced χ^2 of the fits are included as well. For reference, the mean SPE charges are compiled in a table in the Appendix.

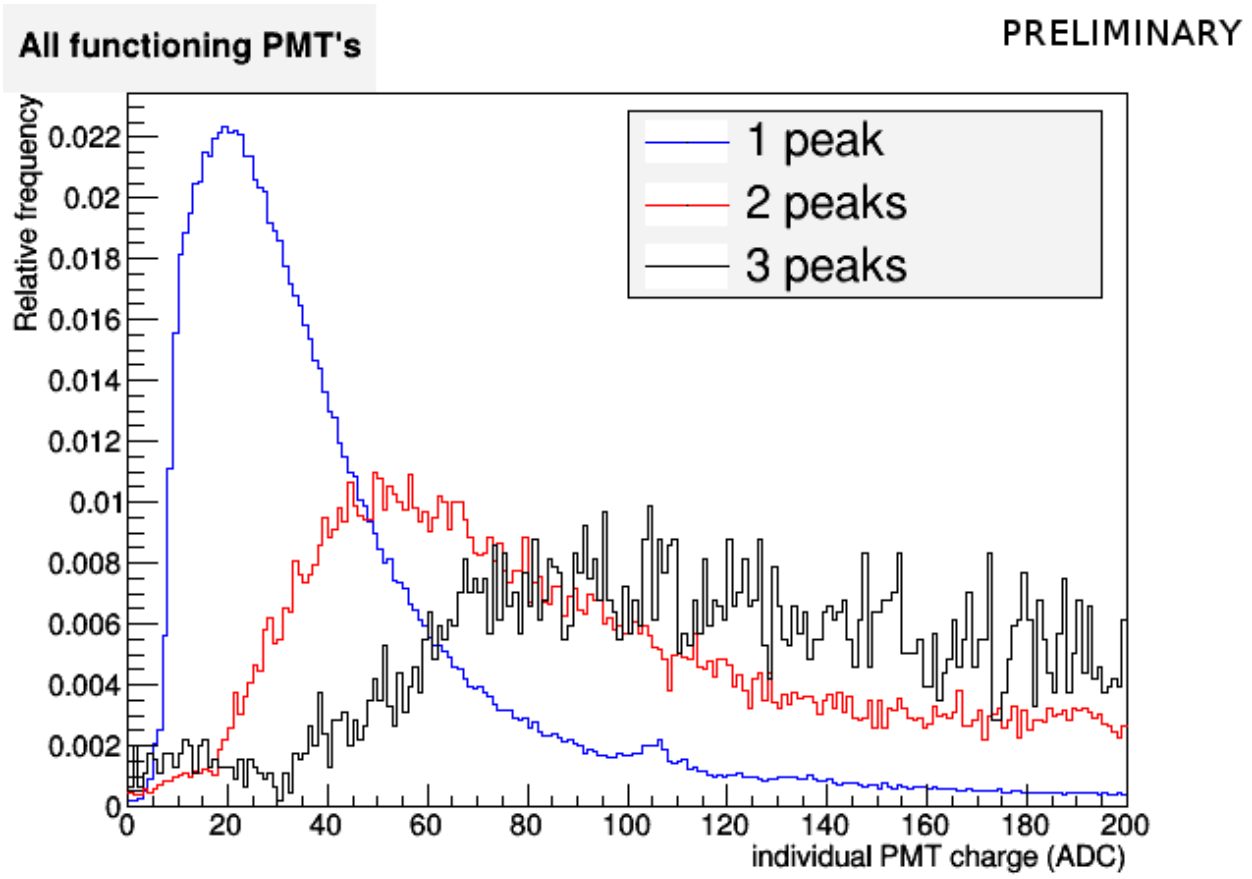

Figure 6: Distribution of charge, over all PMTs, for waveforms with different numbers of peaks.

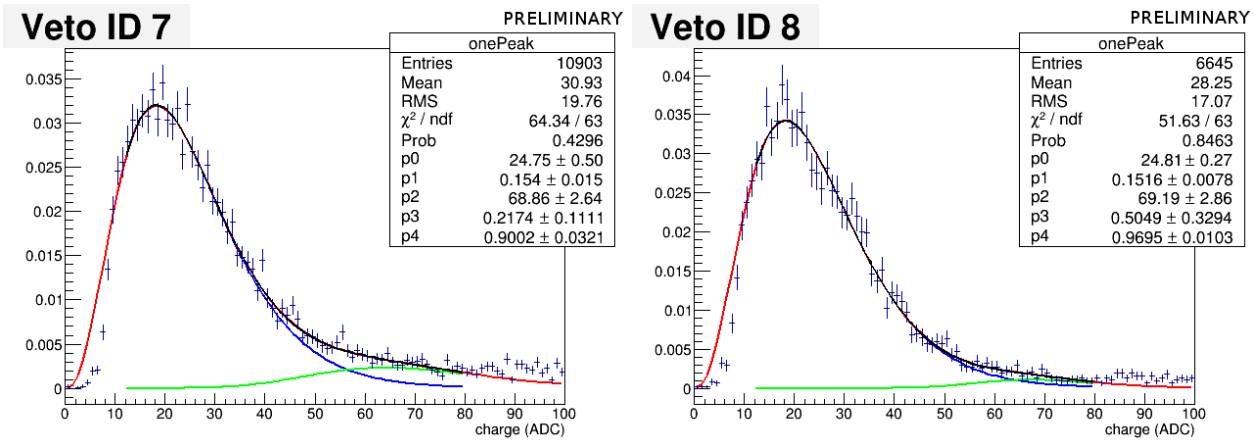

(a) Veto PMT ID 7.

(b) Veto PMT ID 8.

Figure 7: SPE charge distributions for two PMTs fitted to a sum of two gamma distributions. Histograms normalized to a total integral of 1.

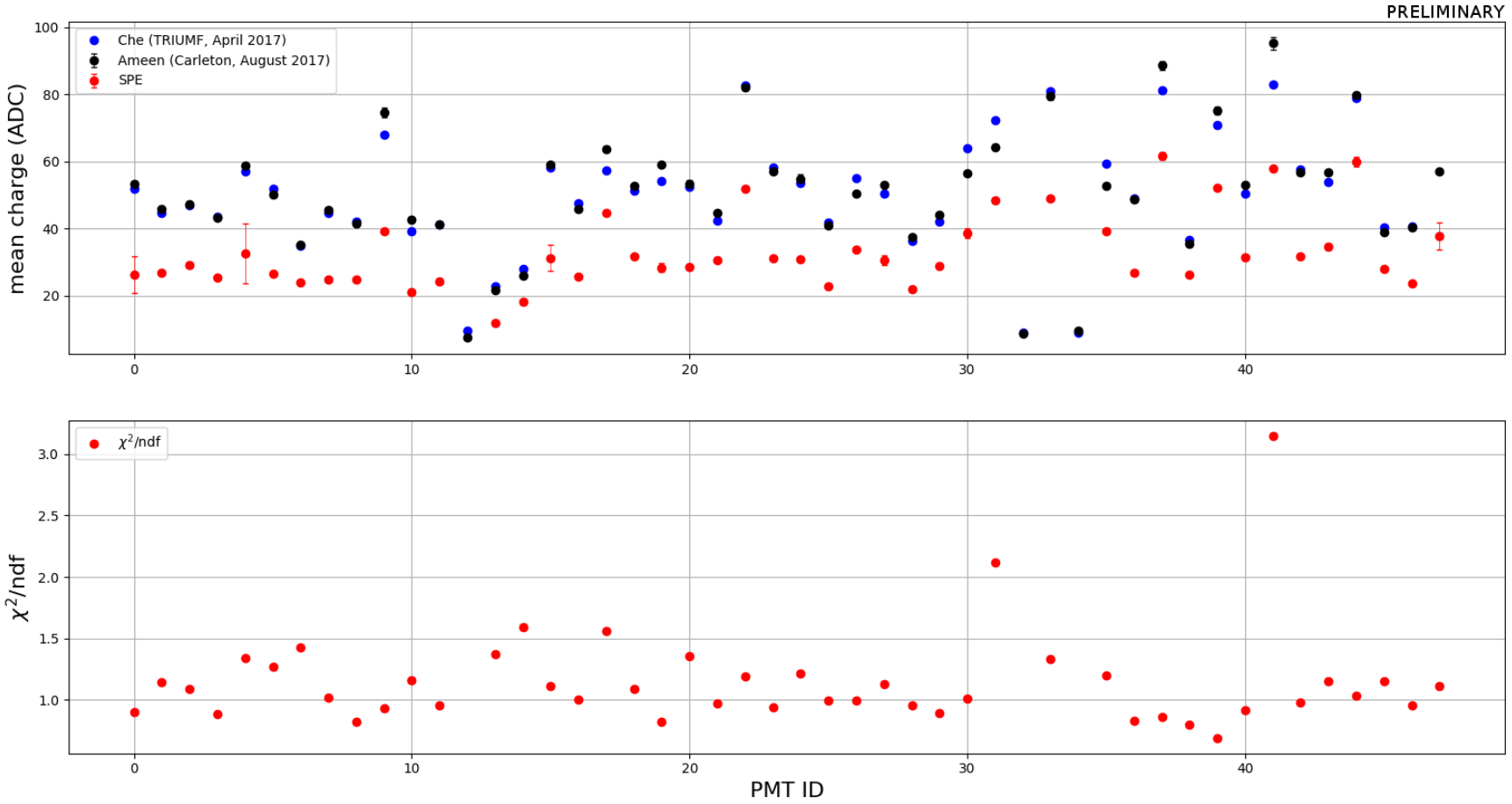

Figure 8: Top: mean SPE charges for each functioning veto PMT and mean charges as determined by Che (using AARF data) and by myself. Bottom: χ^2/ndf for veto PMT fits.

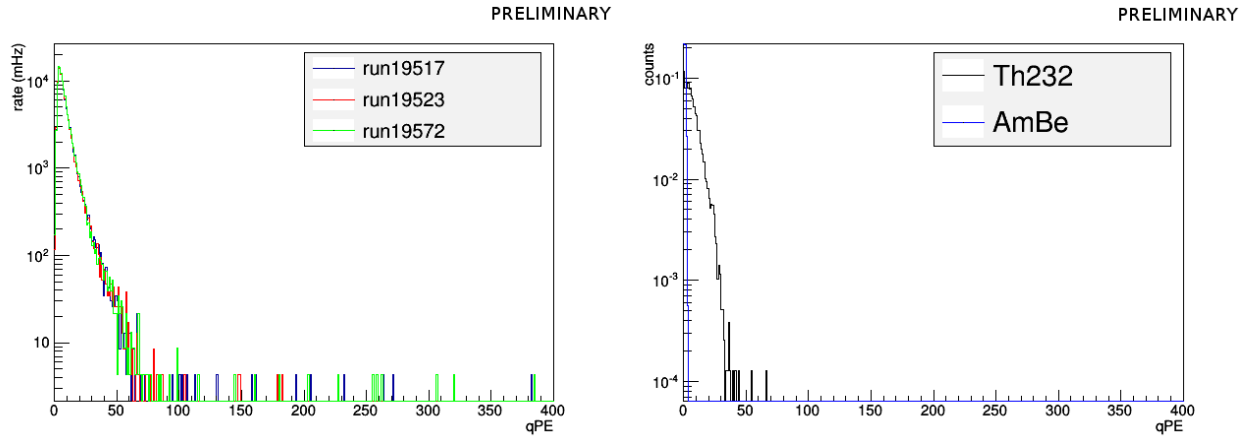

(a) A physics run (19517), ^{232}U run (19523), and ^{22}Na run (19572), normalized for livetime.

(b) Monte Carlo simulations of a ^{232}U run (listed as Th232) and an AmBe run, normalized to an integral of 1.

Figure 9: qPE distributions for three real runs (a) and simulations of two calibration runs (b).

3.4 qPE distributions

qPE distributions for a physics run, ^{22}Na run, and ^{232}U run are overlayed in Figure 9. Also included are qPE distributions for Monte Carlo simulations of a ^{232}U source and an AmBe source. qPE values were calculated using the SPE charges described previously. Each is normalized for livetime, except the simulation.

qPE distributions were also produced for the aforementioned MV events followed by AV events, and for a simulation of 3 GeV electrons. These are provided in Figures 10 and 11, respectively. Note that much higher qPE values are observed than in the previous qPE distributions.

3.5 Event rate

The event rate plots (Figure 12) includes rates for physics runs, AmBe runs, ^{22}Na runs, and ^{232}U runs. Included are plots with a lower bound of 10 and 20 on muonVetoN. The rapid increase in rate starting around run 19350 is due to the cleaning of the water tank. The event rate in calibration runs is similar to that in physics runs.

3.6 Muon follower events

A qPE-fprompt plot of muon events with muonVetoN ≥ 10 that were followed within 1 ms by an AV event was produced (Figure 13). This may be compared to Andrew's similar plot with the older data (see Figure 5.4 in [5]). The two are extremely similar. The time delay between MV and AV events in an event pair were plotted for events with AV_qPE ≥ 50000 (Figure 14). The values are clustered tightly around 4.45 μs.

A similar plot was produced for coincident MV-AV events; i.e. only accepting events that triggered both the MV PMTs and the AV PMTs. This is plotted in figure 15. Also included is a plot of the number of AV PMTs triggered (AV_nhit) against the number of MV PMTs triggered (MV_nhit). There are no coincident events that triggered more than 10 muon veto PMTs, and none with more than about 25000 AV qPE. This is not in agreement with Andrew's results, which is addressed in the next section.

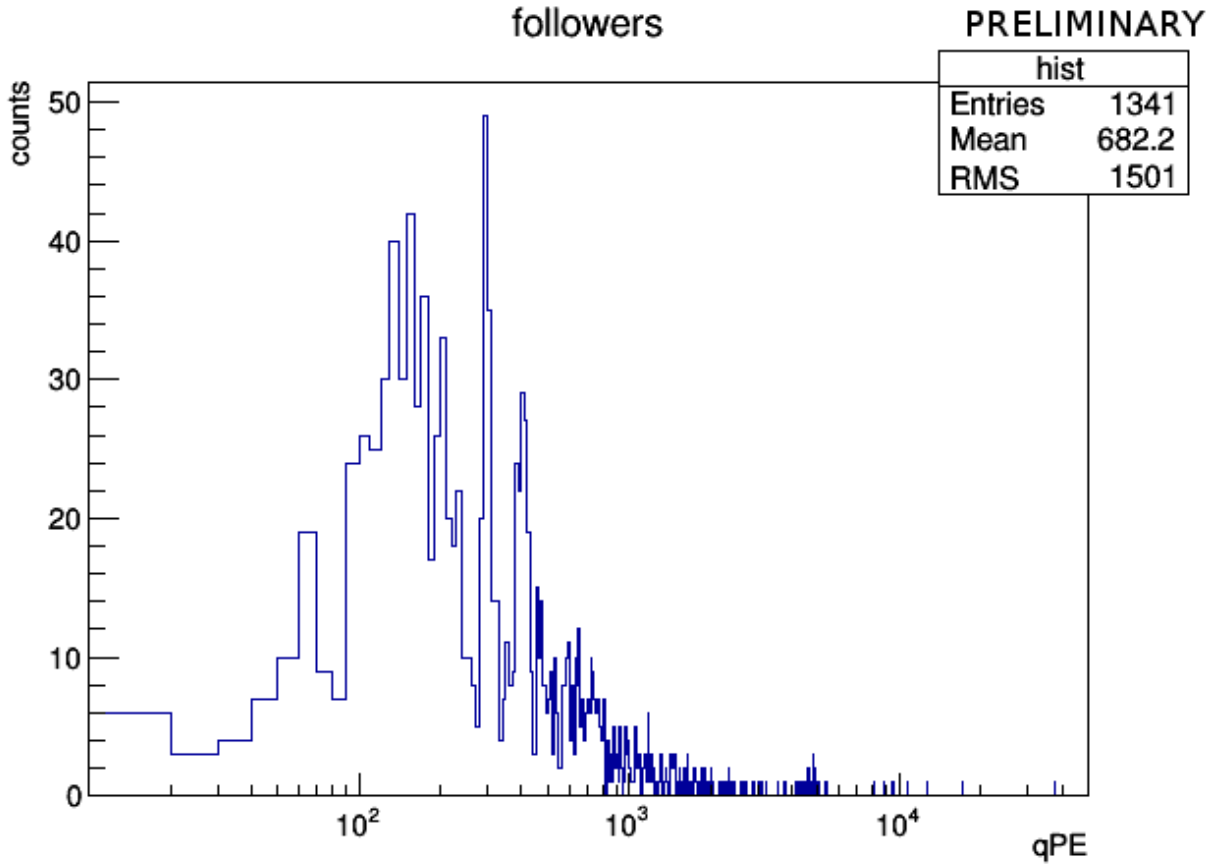

Figure 10: qPE distribution for events that triggered at least 10 muon veto PMTs that were followed by an AV event within 1 ms, and satisfying low level cuts.

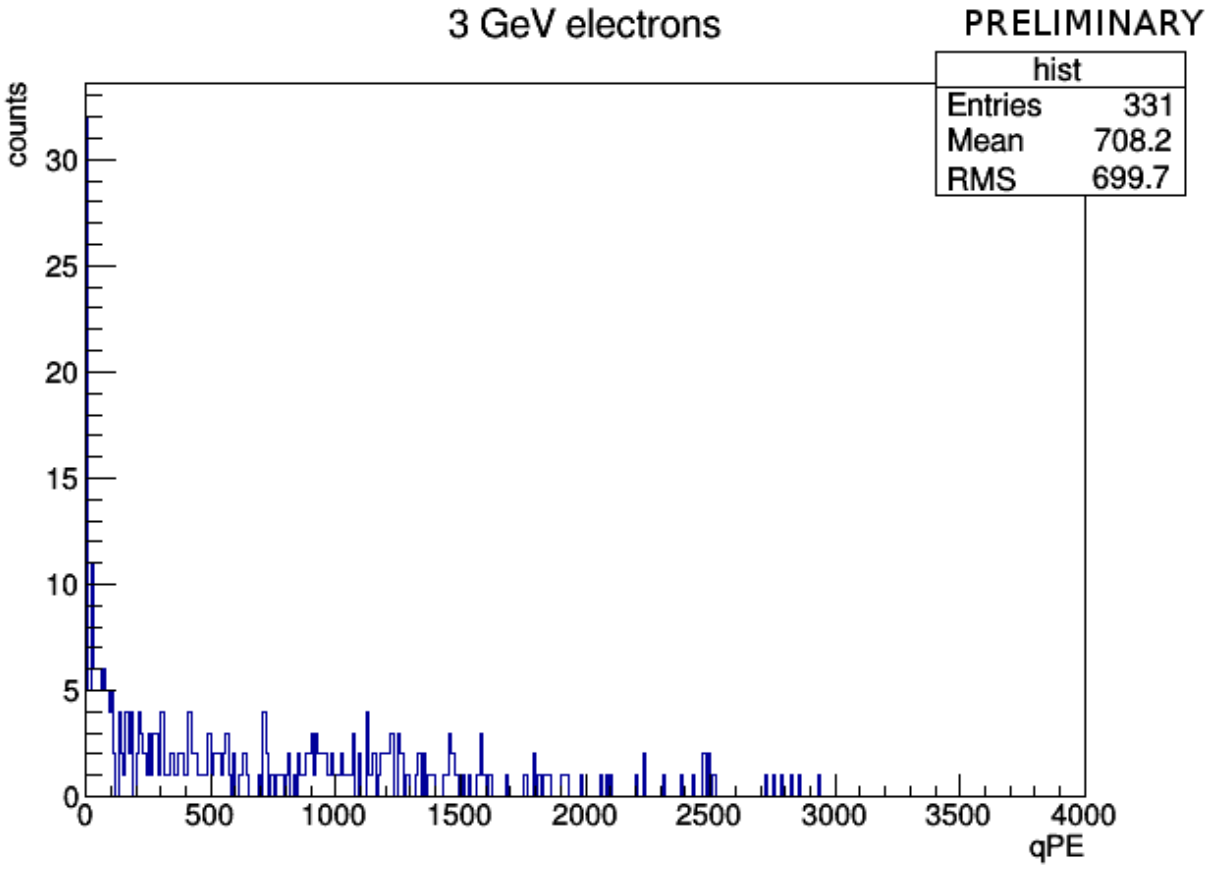

Figure 11: qPE distribution for a simulation of 3 GeV electrons.

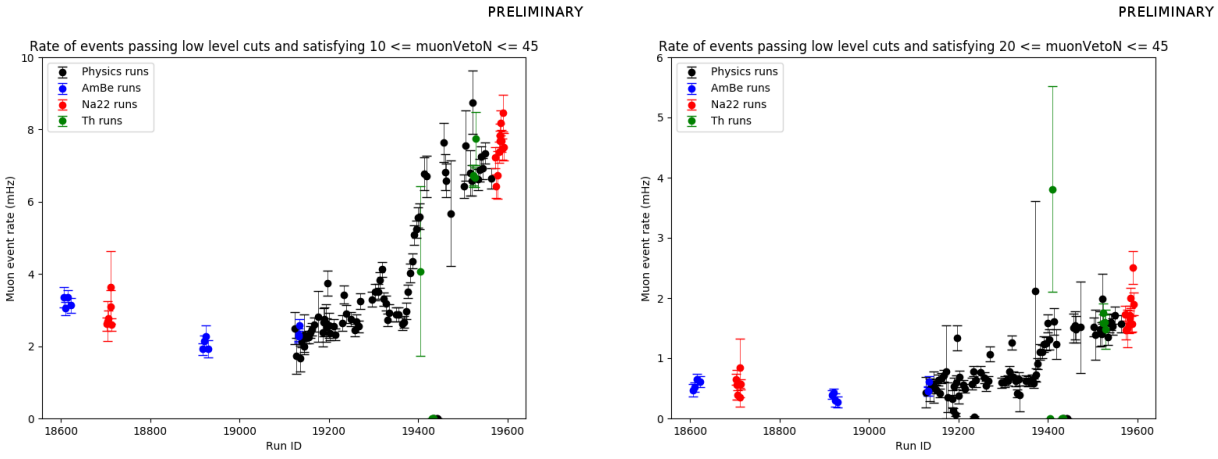

(a) Rate for muonVetoN $\geq$ 10.

(b) Rate for muonVetoN $\geq$ 20.

Figure 12: Rate of muon events with muonVetoN greater than some threshold value and satisfying low level cuts, for various run types. ("Th runs" refers to ^{232}U runs.)

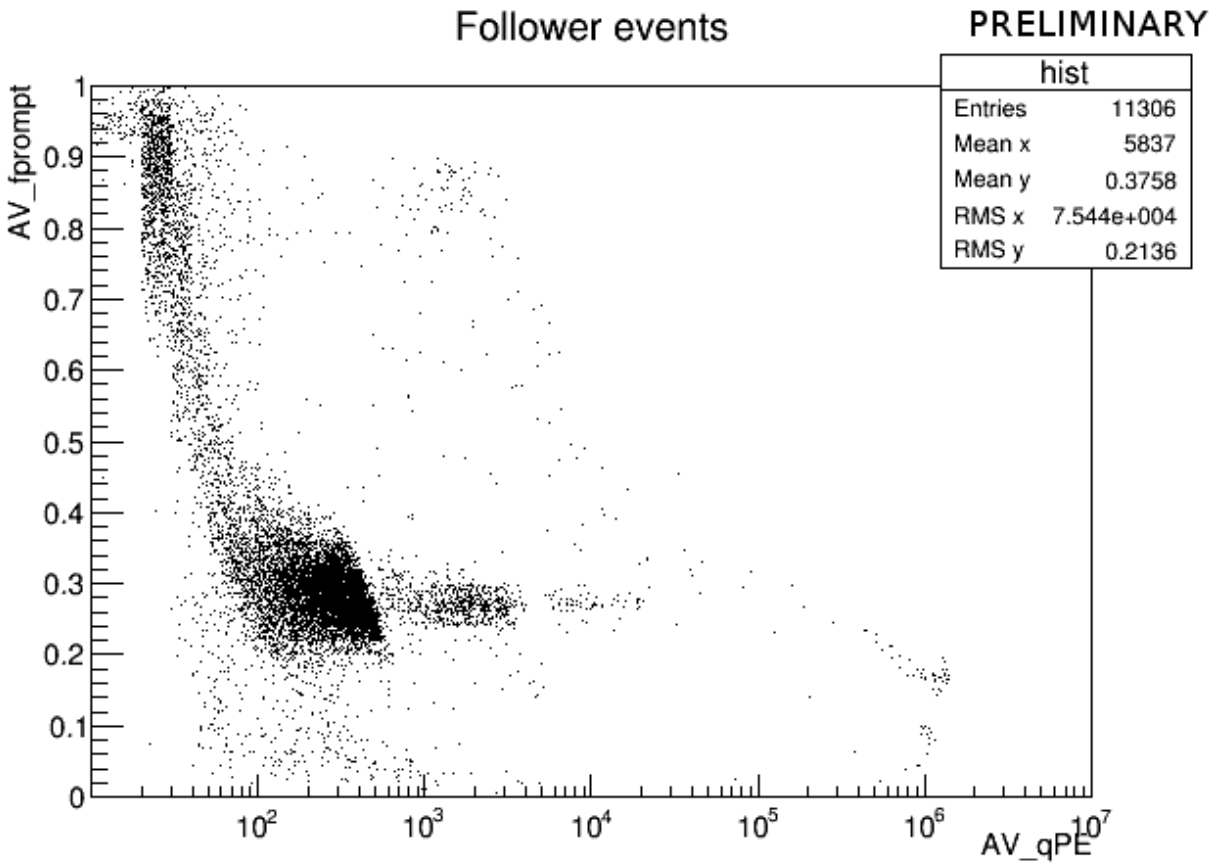

Figure 13: qPE-fprompt distribution of AV events following an MV event.

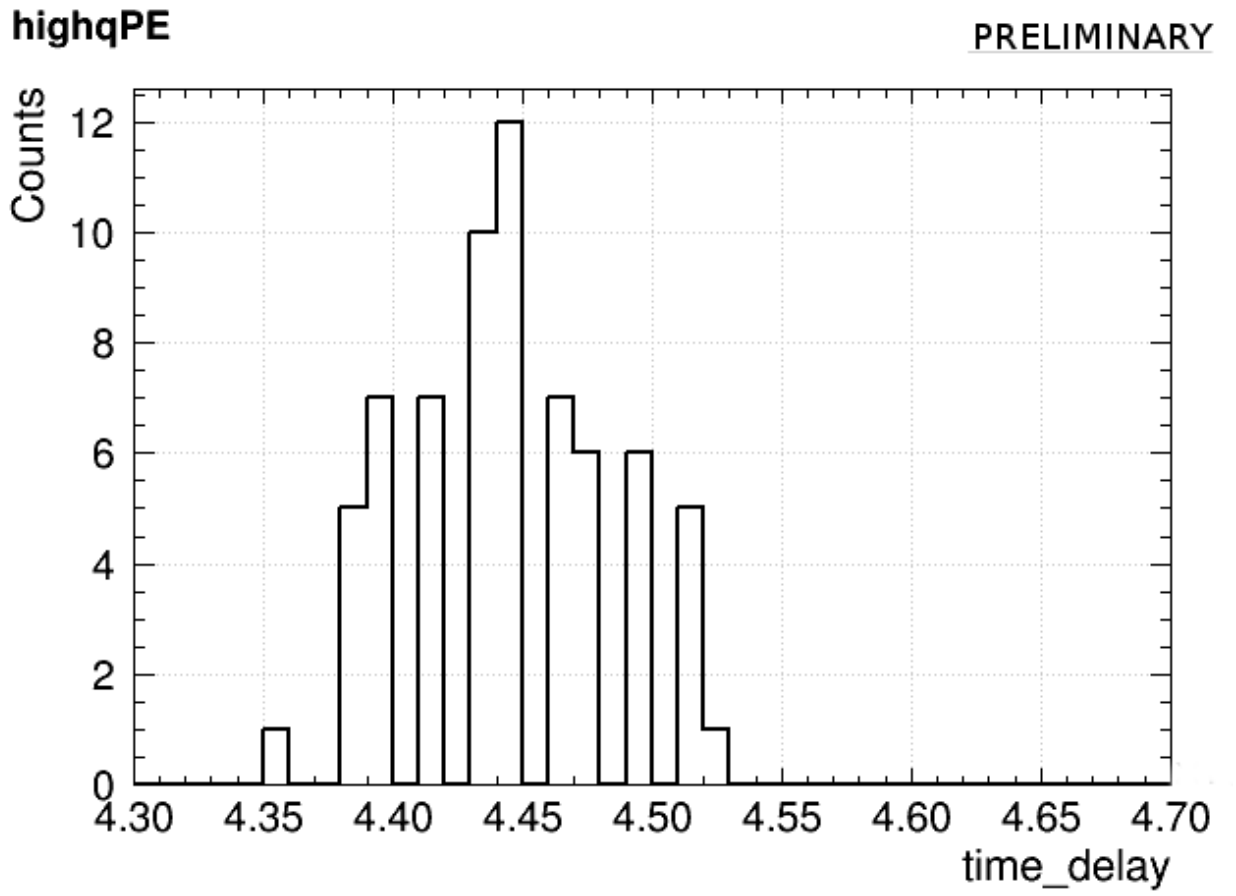

Figure 14: Distribution of time between events in an MV-AV event pair with AV_qPE $\geq$ 50000. x-axis in μs.

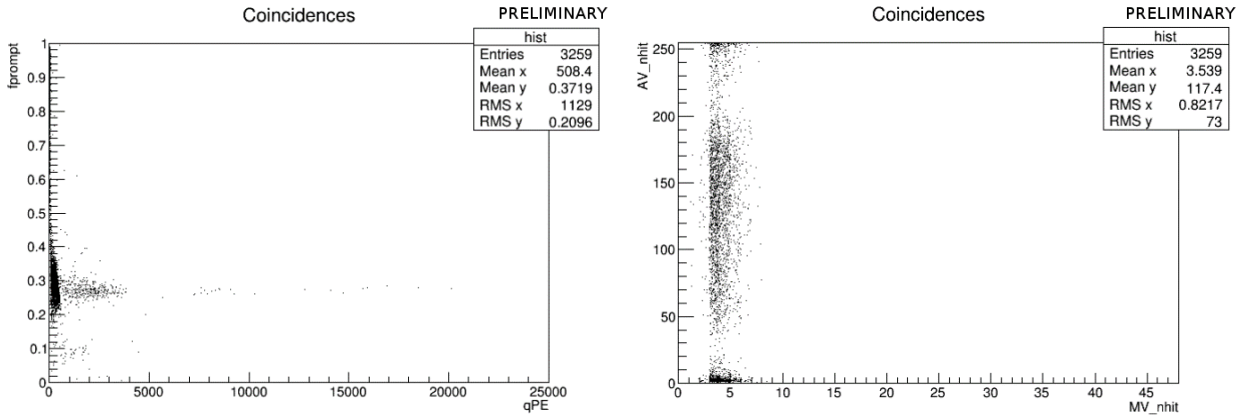

(a) qPE-fprompt distribution for coincident events. qPE here refers to that calculated for the AV PMTs.

(b) AV_nhit (number of AV PMTs triggered) vs. MV_nhit (number of MV PMTs triggered) for coincident events.

Figure 15: Properties of events that simultaneously triggered MV and AV PMTs and satisfy low level cuts.

4 Discussion

The mean baseline waveform value for all functioning PMTs is close to 3900 ADC, as expected. Furthermore, the Gaussian fits have a very small width, on the order of 0.1 ADC. Bear in mind, however, that the fit quality is poor, as evidenced by the large reduced chi-squared values (Figure 2). The RMS of the baseline distributions is similarly small. Andrew explored a preliminary baseline calculation of naïvely averaging the final forty waveform samples, and he found the resulting baseline distributions to be skewed to the left, presumably due to the occasional presence of pulses in those samples [5]. The discrete derivative method employed here eliminates this problem. A reliable baseline calculation is crucial, as charge calculation, and by extension the majority of this report, is dependent on it.

As expected, waveforms with greater charge and/or greater pulse height are more abundant in events with large muonVetoN (Figure 4). An event that triggers more muon veto PMTs is associated with more Cherenkov light in general, so greater pulses are to be expected. One may note a dip around 5-10 ADC in both the charge and height plots of the lowest muonVetoN range. This feature is not fully understood but is likely a threshold effect either at the level of waveform digitizing or at the level of my analysis.

The correlation between charge and height (Figure 5), as well as that between charge and number of waveform peaks (Figure 6), is also unsurprising. The effect of the number of peaks on charge is much more pronounced than that of muonVetoN. There is an unexplained feature in the single peak charge distribution at about 100-110 ADC.

As stated earlier, the cuts used to produce SPE charge distributions were motivated by the charge distributions grouped by muonVetoN and by the number of peaks. These are not the only cuts possible. Over the course of this analysis, it became apparent that some waveforms considerably overshoot the baseline value immediately following the main pulse. This region, where the waveform value is above baseline, reduces the total charge associated with the waveform. Future studies could remove from analysis any waveforms that overshoot the baseline by some arbitrary threshold amount. One will note that the two sample SPE charge fits (Figure 7) do not match the data well below about 10 ADC. This is not all that surprising in light of the aforementioned dip in the charge plot for the lowest muonVetoN range. In fact, the lower bound on the SPE fit region was intentionally chosen to avoid any such threshold effects.

It is fully expected that the mean SPE charges are lower than the mean charges, since the latter is an average over both single-PE and multi-PE events. Indeed, this is consistent with observation (Figure 8). Given this, together with the excellent reduced χ^2 values of the fits, I am quite confident in the validity of these SPE charges.

The qPE distributions produced for the physics, ^{232}U, and ^{22}Na runs are all very similar (Figure 9). This is consistent with the rate of MV events being similar in physics and calibration runs, as evidenced by Figure 12. Interestingly, no events were found with qPE greater than 400. This hints at a lack of real muon signals. This could simply be due to the small sample size of 3×25000 events. But given that the rate of muons passing through the water tank is about 35 per day [5], and that the 25000 events sampled from the physics run correspond to about 3 hours of livetime, it is unlikely that no real muons were observed during this time. This cannot be explained by an issue with the SPE calibration because plenty of extremely high-qPE events are observed for events followed by an AV event (Figure 10). It would be worthwhile to produce qPE distributions with much larger sample sizes.

The simulated qPE distribution for a ^{232}U source seems similar to the actual ^{2}32U qPE distribution. The simulated distribution may fall off more rapidly. The AmBe simulated distribution does not look like the others. There is a curious lack of events with even moderately high qPE ($\sim$100) in either distribution. Sample size is not the issue: 2 million gamma rays were fired for the ^{232}U simulation and 1 million for the AmBe simulation. Notably, qPE values ranging up to a few thousand were observed in a simulation of only 1000 3 GeV electrons (Figure 11). This phenomenon was not fully explored due to time constraints; further investigation is certainly required.

Again, the event rate plots (Figure 12) are consistent with the qPE distributions in that calibration runs and physics runs have similar rates. The rapid rise in event rate is fully explained by the cleaning of the water tank. There are a few runs with a rate of 0, which simply correspond to runs where the muon veto system was not operational. Andrew, analyzing older data, noted four runs with anomalously high muon event rates, and concluded that the veto system was likely malfunctioning during these runs [5]. No such runs were observed in the newer data, indicating good functioning of the muon veto system.

The qPE-fprompt plot for muon follower events (Figure 13 is in good agreement with Andrew's plot. However, in Figure 15, where the analysis is restricted to coincident MV-AV events, the situation is different. No events with qPE (AV_qPE, that is) greater than 25000 or muonVetoN greater than 10 were observed in the data from Nov. 2016 to Apr. 2017. This is in stark contrast to Andrew's analysis of older data, which found 28 coincident events with qPE $\geq$ 50000, all but one of which had muonVetoN $\geq$ 39 [5]. Such high-qPE events are not absent from general muon follower events. This is most probably explained by a change in the way data is stored. This possibility was not investigated further due to time constraints.

The time delay in MV-AV event pairs with high AV_qPE (Figure 14) is restricted to a narrow band entirely contained between 4.30 and 4.60 μs, with a peak at 4.45 μs. These are similar to the time delays Andrew found for three candidate muon-induced follower events with AV_qPE about 10^6. A possible next step would be to produce time delay distributions for different, lower AV_qPE regions. With the MV SPE calibration introduced in this work, it would even be feasible to produce such distributions for different MV_qPE regions.

To summarize, SPE charge distributions were produced for the muon veto PMTs and fitted to a model. SPE charges were extracted from the fits. Based on the various charge distributions produced and the cuts they motivated, the comparison of SPE charges to mean charges, and the quality of the SPE fits, I have good reason to believe these SPE charges are reliable. There is much work to be done with respect to qPE distributions. In particular, the lack of high-qPE events and the strange shape of the AmBe simulated qPE distribution must be explained.

References

[1] P.-A. Amaudruz *et al.* (DEAP collaboration). "In-situ characterization methods for the Hamamatsu R5912 photomultiplier tubes used in the DEAP-3600 experiment." arXiv:1705.10183.

[2] M.G. Boulay (for the DEAP collaboration). "DEAP-3600 dark matter search at SNOLAB." *J. Phys. Conf. Ser.* 375. 2012.

[3] C. Geofroy, "Veto PMT analysis for DEAP-3600." Internal report. TRIUMF. Vancouver, BC, Canada. 2017.

[4] R. Stainforth. "Cuts and Acceptances." DEAP-STR-2017-013 (2013).

[5] A. Zwaniga. "Studies of the muon veto detector for the DEAP-3600 experiment." Undergraduate thesis. Department of Physics. Carleton University. Ottawa, ON, Canada. 2017.

A Table of SPE Charges

Table 1: SPE charges for each functioning muon veto PMT. See Methods and Results for explanations of how these were calculated.

Veto PMT ID	SPE charge (ADC)	Veto PMT ID	SPE charge (ADC)
0	26.2 ± 5.4	24	30.94 ± 0.25
1	26.85 ± 0.29	25	22.64 ± 0.67
2	29.08 ± 0.82	26	33.60 ± 0.29
3	25.42 ± 0.31	27	30.6 ± 1.5
4	32.5 ± 8.9	28	21.83 ± 0.16
5	26.59 ± 0.29	29	28.83 ± 0.22
6	24.06 ± 0.22	30	38.6 ± 1.4
7	24.75 ± 0.50	31	48.37 ± 0.65
8	24.81 ± 0.27	32	malfunctioning
9	39.32 ± 0.47	33	48.92 ± 0.47
10	21.03 ± 0.24	34	malfunctioning
11	24.24 ± 0.23	35	39.12 ± 0.34
12	malfunctioning	36	26.94 ± 0.22
13	11.98 ± 0.14	37	61.6 ± 1.2
14	18.07 ± 0.73	38	26.36 ± 0.20
15	31.25 ± 3.79	39	52.08 ± 0.58
16	25.76 ± 0.39	40	31.47 ± 0.48
17	44.58 ± 0.43	41	57.90 ± 0.58
18	31.82 ± 0.56	42	31.65 ± 0.28
19	28.4 ± 1.4	43	34.55 ± 0.94
20	28.54 ± 0.45	44	58.0 ± 1.5
21	30.62 ± 0.32	45	28.08 ± 0.26
22	51.72 ± 0.66	46	23.68 ± 0.22
23	31.15 ± 0.63	47	37.7 ± 4.0